Oscillatory behavior of 5*d* magnetic moments in Fe/W multilayers

N. Jaouen,[1] G. van der Laan,[2] T. K. Johal,[2] F. Wilhelm,[1] A. Rogalev,[1] S. Mylonas,[3] and L. Ortega[4]
[1]*European Synchrotron Radiation Facility, B.P. 220, F-38043 Grenoble Cédex, France*
[2]*Magnetic Spectroscopy, Daresbury Laboratory, Warrington, WA4 4AD, United Kingdom*
[3]*Laboratoire de Métallurgie Physique, Université de Poitiers, 86962 Futuroscope Chasseneuil, France*
[4]*Laboratoire de Cristallographie, CNRS Grenoble, France*
(Received 20 May 2004; published 22 September 2004)

We used x-ray resonant magnetic scattering (XRMS) across the W L_3 absorption edge in combination with x-ray magnetic circular dichroism and anomalous x-ray reflectivity to obtain the magnetic polarization profile in a Fe(30 Å)/W(11 Å) multilayer. This extends the use of XRMS to the 5*d* transition metals for the study of induced magnetization. Analysis of our experimental results shows that there is a strong oscillatory behavior of the magnetization in the W layer. This tendency is in good agreement with the recent theoretical predictions by Tyer *et al.* [Phys. Rev. B **67**, 104409 (2003)].

DOI: 10.1103/PhysRevB.70.094417 PACS number(s): 75.70.Cn, 78.70.Ck, 78.70.Dm

I. INTRODUCTION

Driven by the unique properties of synchrotron radiation and progress in materials science in supplying materials with ever increasing complexity, scientific interest in the use of x-ray scattering to determine the magnetic structure and orbital ordering has significantly grown over the last few years. Traditionally, x-ray reflectivity measurements have been used to determine structural information, such as layer thickness, effective electron density, and interfacial roughness. However, conventional x-ray reflectivity is limited when it comes to separating structural parameters for layers of different elements in the Periodic Table. One way to enhance the chemical contrast is to take advantage of the tunability of the incident photon energy using synchrotron radiation. Close to an absorption edge of an atom the scattering factor is resonantly enhanced. Moreover, by using polarized x rays the resonant scattering becomes sensitive to the magnetization profile in the material.

X-ray magnetic scattering experiments were pioneered by de Bergevin and Brunel on NiO using a tube source.[1] Early calculations by Blume[2] showed that resonance effects occur near an absorption edge and a very small effect was indeed observed by Namikawa *et al.*[3] in ferromagnetic Ni by tuning the incident x-ray energy to the *K* edge. Large resonant enhancements of the magnetic scattering were discovered at the $L_{2,3}$ edges of the rare earths[4] and the $M_{4,5}$ edges of the actinides,[5] which could be explained in terms of atomic physics.[6] Strong magnetic dichroism was predicted[7] and, soon after, observed[8] in x-ray absorption (i.e., forward scattering) proportional to the element-specific magnetic moment. Thus, x-ray resonant magnetic scattering (XRMS) combines the advantages of magnetic x ray dichroism with those of x-ray scattering. Although soft x rays usually have prohibitively long wavelengths for Bragg diffraction from crystal lattices, in 3*d* transition metals the wavelength of the $L_{2,3}$ absorption edges[9] matches perfectly onto the nanometric length scale of artificial multilayers[10] and periodic domain structures.[11]

Despite the extraordinary potential of such an approach for studying magnetic nanostructures, only a few scattering experiments have been reported so far in the hard x-ray range, and these concerned rare-earth elements,[12–14] where the localized 4*f* electrons play a key role in the magnetic properties and strongly influence the 5*d* valence electrons. A previous study[13] reports on the study of the magnetic structure of Ce through the γ to α phase transition. An oscillating profile was found for α-Ce and a simple decreasing profile for γ-Ce. It is known that the α-Ce (Ce/Fe) ground state is a mixture of $4f^1$ and $4f^0$ states with a strong hybridization between the 4*f* state and the valence electrons, which plays a key role in the properties of such Ce based system. In the γ phase, the ground state is a well-localized $4f^1$ state, and the behavior resembles a normal metallic system. Therefore, the logical conclusion of this study[13] was that the oscillating behavior is strongly related to the presence of mixed-valence 4*f* states, which strongly interact with the 5*d* band.

In this paper we report the magnetic behavior of W in a Fe/W multilayer, where only the 5*d* conduction electrons are of importance, which gives a completely different physical mechanism for the magnetism than in the case of Ce. An oscillating behavior of the W magnetic moment has recently been predicted in Fe/W multilayers.[15] Electron hybridization at interfaces can change the spin magnetic moments of the magnetic layers and induce magnetization in adjacent "nonmagnetic" layers.[15] In giant magnetoresistive (GMR) materials, such as Fe/Cr multilayers, the magnetic layers are (anti)ferromagnetically coupled by the Ruderman-Kittel-Kasuya-Yosida (RKKY) interaction, which induces an oscillatory spin magnetic moment in the nonmagnetic layer. However, experimental evidence for an oscillatory spin behavior in Fe/W is so far lacking. Furthermore, such systems that combine a large 3*d* spin moment with a strong 5*d* spin-orbit interaction are of special interest because of their enhanced magneto-optical response.

Improved understanding of the mechanism giving rise to magnetic interaction in multilayered systems can be gained by studying directly the induced magnetic properties of the

nonmagnetic constituent near the interface. Recent x-ray magnetic circular dichroism (XMCD) studies at the W $L_{2,3}$ absorption edge, probing specifically the 5*d* valence states in Fe/W multilayers, evidenced a significant induced magnetic moment in an ultrathin W spacer layer.[16] However, XMCD only gives the magnetic moments averaged over all W layers (properly corrected for the sampling depth). XRMS would give the layer-resolved magnetic moments if we are able to detect the magnetic contribution to the different order Bragg peaks using circular dichroism.[12–14] In the particular case of Fe/W, the line shape of the W L_3 XMCD gives a characteristic signature of the magnetic polarization,[16] so that the energy dependence of the asymmetry ratio for the different Bragg peaks can be used to provide a probe for the profile of the magnetic polarization. Furthermore, measurement of the intensity at the Bragg peaks, which originate from the interference process between periodically stacked layers, strongly reduces the influence of the capping layer, buffer layer and substrate.

The outline of this paper is as follows. In Sec. II we describe the sample preparation and the structural characterization of the Fe/W multilayer. We present experimental results using x-ray diffraction (XRD), XMCD, and XRMS. In Sec. III we briefly explain the data analysis of the XRMS results, which can give the layer resolved induced magnetization within the W layer. The obtained results are discussed in Sec. IV and compared to those from recent band-structure calculations. Finally, conclusions are drawn in Sec. V.

II. EXPERIMENTAL RESULTS

The Fe/W multilayer for this study was grown in a computer-controlled ion-beam Nordiko™ 3000 sputtering system equipped with two rf-excited filamentless guns and filamentless cold-cathodes for plasma neutralization. A sapphire $(1\bar{1}20)$ substrate was fixed on a rotating substrate holder that included a heating stage. Prior to the multilayer deposition, a 4 nm Mo buffer layer was deposited at 1020 K in order to favor epitaxial growth. The anticipated thicknesses for the Fe and W layers were 30 and 10 Å, respectively. A total of 25 alternating layers was deposited giving a nominal multilayer thickness of 100 nm.

The structural characterization of the multilayer has been performed with high-angle XRD using a conventional Cu rotating anode source and proportional counter. A graphite monochromator was used to select the Cu $K\alpha$ radiation. The measurements were performed in the symmetric reflection geometry at ambient temperature. In order to extract the lattice parameter required for the XRMS analysis, the measured spectra were fitted by using a modified version of the superlattice refinement code SUPREX.[17] The position of the main diffraction peak gives directly the average *d* spacing and the multilayer period. The fitting algorithm is used to reproduce the entire XRD pattern, i.e., the peaks positions, relative intensities and lines profiles. The best-fit curve (solid line) is shown in Fig. 1 together with the experimental curve (dashed line). A rather good overall agreement is observed except for the main peak arising from the sapphire substrate that has not been included in our calculations. The slightly higher intensity of the high-order satellite peaks could be assigned to a lack of coherence through the entire multilayer stacking which was not taken into account in our simulation. The results of the XRD analysis for the Fe(30 Å)/W(11 Å) multilayer are the following: the texture is (110) with *d* spacings (normal to the layers) of $d_{Fe}=2.06$ Å (bulk like) and $d_W=2.235$ Å. In order to account for the important Fe and W lattice mismatch of 9.4%, two atomic planes were allowed to expand or contract at the bottom and the top of each layer assuming an exponential profile. The result of the fit indicates a relative expansion of 0.12 Å for d_W and a contraction of 0.07 Å for d_{Fe} following this exponential law. Simultaneously, to compensate for this behavior, according to the elastic theory, the best-fit of the measured XRD profile was obtained with a 5% increase of the in-plane density for the W layers (lattice contraction) and a mandatory 5% reduction of the in-plane density of the two first Fe planes at the interface (lattice expansion). In agreement with the thicknesses of the W and Fe layer, we found that the whole W layer is constrained.

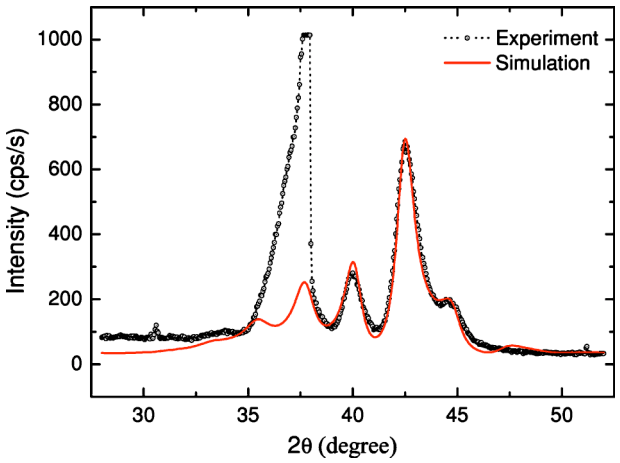

FIG. 1. (Color online) X-ray diffraction (black dashed line with dots) measured with Cu $K\alpha$ source (1.54 Å) together with simulation (red drawn line), see text for details.

Anomalous reflectivity, XRMS and XMCD experiments were carried out using 95% circularly polarized x rays from beamline ID12 of the European Synchrotron Radiation Facility (ESRF) at Grenoble. For the XMCD measurements the sample was mounted at grazing incidence in the bore of a 7 Tesla superconducting magnet. Anomalous reflectivity and XRMS were measured using a UHV two-circle reflectometer at low grazing incidence angles θ of the x rays. The sample was magnetically saturated using a rotatable array of permanent magnets producing a field of 0.5 Tesla, which was applied along the intercept of the sample surface and the diffraction plane. A field of few hundred G is sufficient to fully saturate the sample. In order to avoid any experimental artifacts, the XMCD and XRMS were recorded by reversing the photon helicity vector as well as by reversing the direction of applied magnetic field. All data have been corrected for the incomplete degree of circular polarization. The beamline quality combined with a high efficiency of the detection system[18] allowed us to extract the very low asymmetry ratios with good signal-to-noise ratio ($\leqslant 2\times 10^{-4}$). While prior to

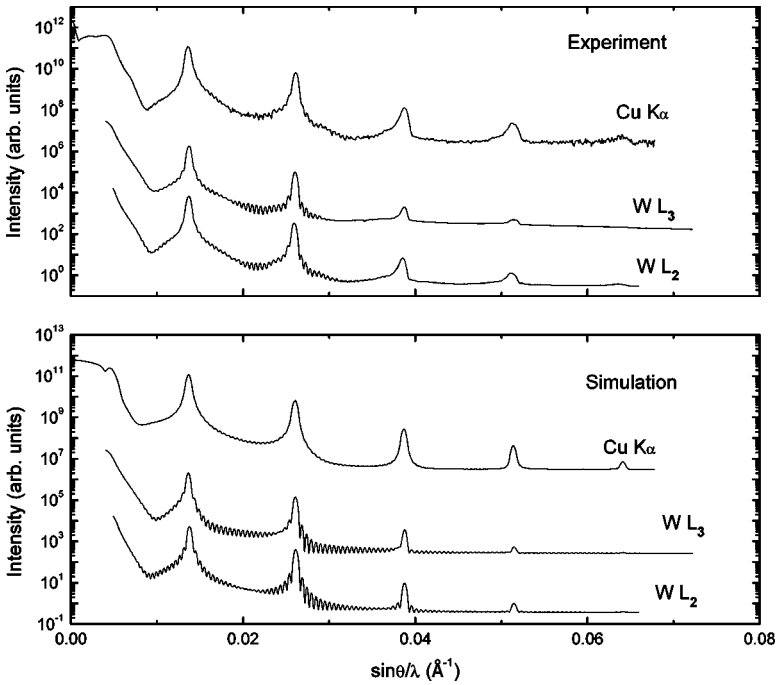

FIG. 2. Upper panel: X-ray reflectivity measured with Cu $K\alpha$ source (1.54 Å) and at resonance with the W L_3 (1.21 Å) and W L_2 (1.07 Å) absorption edges. Lower panel: Simulation, see text for details.

the experiments the quality of the stacking of the superlattice was properly checked using a Cu $K\alpha$ source, we also recorded the anomalous reflectivity at the photon energies of the W L_2 and L_3 edges, showing a superior signal-to-noise ratio, as is seen in Fig. 2. The reflectivity curves contain distinct Bragg peaks separated by $\sin\theta/\lambda \approx 0.013$ Å^{-1}, corresponding to the Fe/W period. The first four Bragg peaks are very prominent while the fifth peak starts to submerge in the background. There are also short-period oscillations, known as Kiessig fringes, arising from the interference between the scattering amplitudes from top and bottom of the multilayer stack. There are indeed 25 oscillations between adjacent Bragg peaks, corresponding to the number of periods. The experimental curves were refined using a modified version of the SUPREX package.[17] Figure 2 illustrates the good agreement between the experimental and simulated results, which are consistent with a thickness of 29.7 Å and 11.4 Å for the Fe and W layers, respectively. Furthermore, an interdiffusion corresponding to two atomic plane at each interface was obtained, in good agreement with the high-angle diffraction results.

Figure 3 shows the XAS and XMCD recorded at the W L_3 edges of the Fe/W multilayer at $T=300$ K and $H=4$ T. Despite its very small amplitude (multiplied by 50 for clarity in Fig. 3) a clear XMCD signal was detected assuring the presence of a nonvanishing induced magnetization in the W 5*d* states. The XMCD spectrum agrees well with the shape measured previously on a similar sample[16] but was smaller in magnitude due to the thicker W layer. Applying the magneto-optical sum rules[19,20] to the measured W $L_{2,3}$ edges gives an average total 5*d* magnetic moment $\mu_{av}=-0.038\ \mu_B$/atom and an orbital-to-spin magnetic moment ratio of 0.085.

The layer-resolved magnetization can be obtained by analysing the XRMS of all of the four distinct Bragg peaks. Figure 4 shows the energy dependence of the asymmetry ratio $R=(I^+-I^-)/(I^++I^-)$ across the W L_3 edge measured on top of the Bragg peaks, where I^+ and I^- are the diffracted intensities for opposite alignments between magnetic field and photon helicity. The strongly different energy dependence of R for each Bragg peak is a direct indication that the magnetic polarization is not constant throughout the W layer.

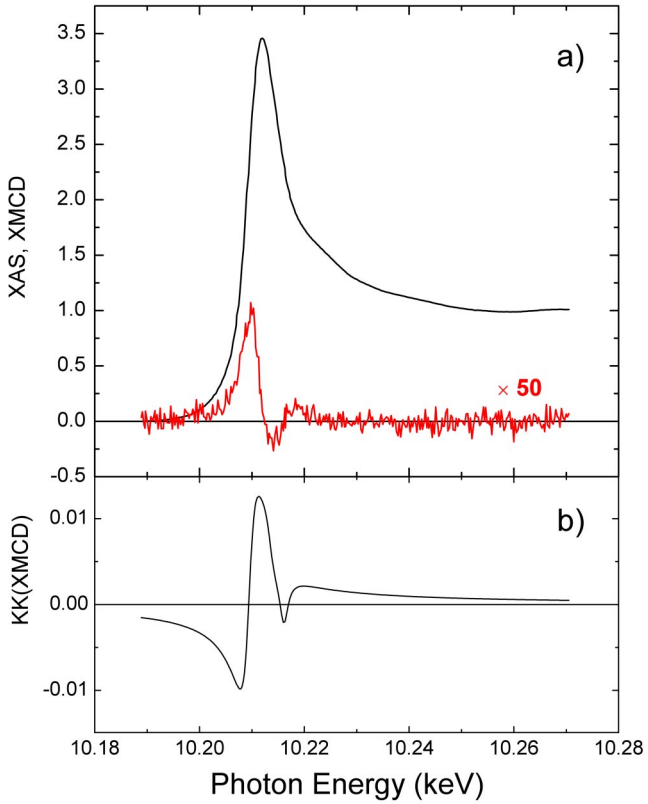

FIG. 3. (Color online) (a) XAS and XMCD (red) recorded at the W L_3 edge; (b) real part (m') of the magnetic scattering factor calculated as the Kramers-Kronig transform of the XMCD.

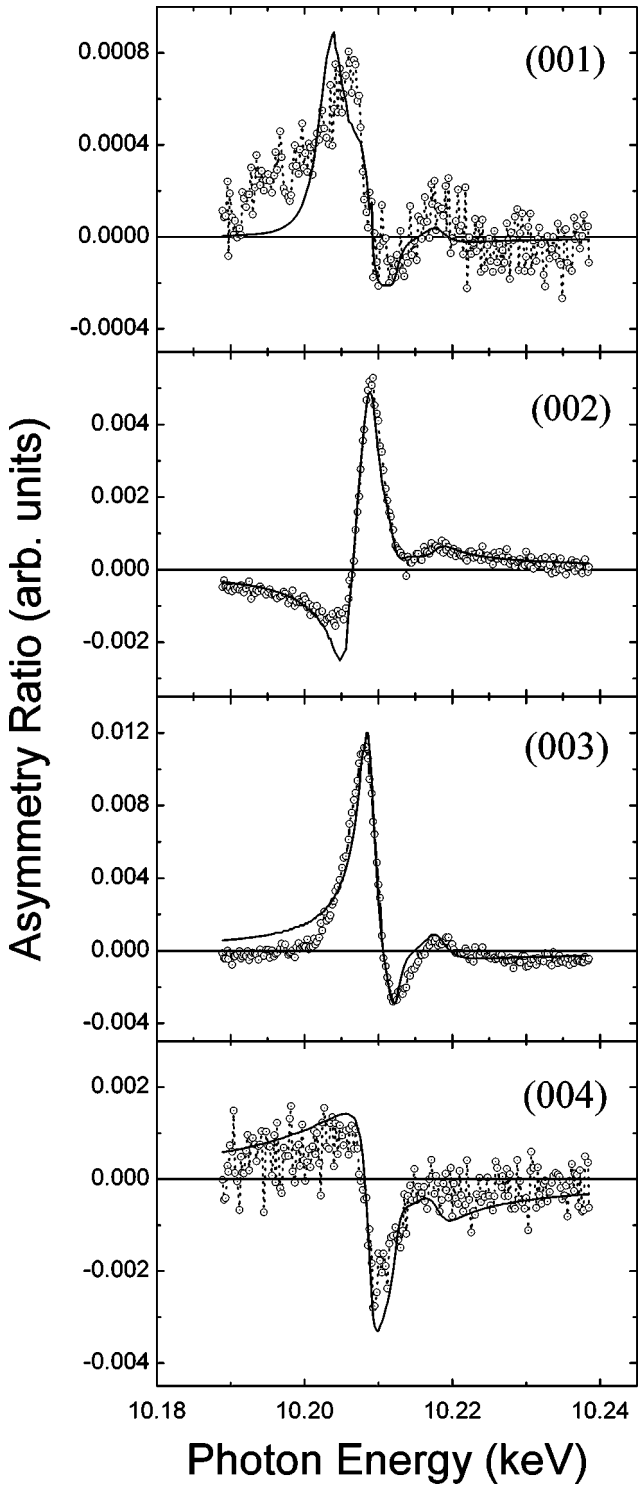

FIG. 4. X-ray resonant magnetic scattering results. Energy dependence of the asymmetry ratio, R, measured for the first four low-order Bragg peaks across the W L_3 edge. Experimental (open circles) and calculated curves (drawn lines) leading to the magnetic profile given in Table I.

These variations could only be observed because of the sufficiently small energy step in the measurement (0.25 eV) associated with the high stability of the x-ray beam. If the asymmetry ratio would have displayed the same shape for each diffraction order, then both the charge and the magnetic structure factors have the same q dependence.

III. ANALYSIS METHOD

In order to explain how the magnetization profile can be extracted from the XRMS, we briefly outline the theoretical interpretation of the spectra. To first order in the magnetization, the atomic scattering factor can be written as[6]

$$f(E) = (\hat{\mathbf{e}}_f^* \cdot \hat{\mathbf{e}}_i)F^0(E) - i(\hat{\mathbf{e}}_f^* \times \hat{\mathbf{e}}_i) \cdot \hat{\mathbf{z}}F^1(E),$$

with the charge and magnetization dependent scattering amplitudes

$$F^0(E) = f_0 + f'(E) - if''(E),$$

$$F^1(E) = m'(E) - im''(E),$$

respectively, where E is the energy of the incident x-rays, $\hat{\mathbf{e}}_i$ and $\hat{\mathbf{e}}_f$ are the unit polarization vectors of the electric field for the incident and scattered x rays, respectively, and $\hat{\mathbf{z}}$ is the magnetization unit vector. f_0 is the regular charge scattering factor and f' and f'' are the energy-dependent resonant contributions associated with the absorption edge. m'' is the imaginary part of the forward scattering, which is directly obtained from the XMCD. m' is derived from m'' by using the Kramers-Kronig relation and the result is displayed in Fig. 3(b).

Away from the critical angle, the first Born approximation remains valid, and we can define the complex charge and magnetic structure factors,

$$F(\mathbf{q},E) = F' - iF'' = \sum_j C_j\sigma_j F^0(E)e^{i\mathbf{q}\cdot\mathbf{r}_j},$$

$$M(\mathbf{q},E) = M' - iM'' = \sum_j \frac{C_j\mu_j}{\mu_{\mathrm{av}}}\sigma_j F^1(E)e^{i\mathbf{q}\cdot\mathbf{r}_j},$$

respectively, where j runs over the different layers, whose composition, especially in the interface region, may be altered by changing the concentration C_j of the different atomic species. σ_j corresponds to the planar atomic density divided by the layer thickness, μ_j is the magnetic moment per atom. The average magnetic moment $\mu_{\mathrm{av}} \equiv \Sigma_j C_j\mu_j/\Sigma_j C_j$ is obtained from the XMCD. In the complex structure factor, $\mathbf{r}_j$ gives the position of the layers and $\mathbf{q}$ the scattering vector perpendicular to the surface. Since the XRMS is sensitive to $C_j\mu_j$/atom, x-ray reflectivity measurements are required to find C_j. Therefore, the real structure characterization of the sample is an important prerequisite for the analysis of the XRMS. The element-specific magnetic profile is obtained using a refinement procedure[12,13] that calculates the energy dependence of the asymmetry ratio, R, which for a longitudinal geometry and circular polarization can be written as[21]

$$R = \frac{-2\cos^3\theta\,(F'M' - F''M'')}{1 - \frac{1}{2}\sin^2 2\theta\,|F^2| + \cos^2\theta\,|M^2|}.$$

Details about the refinement procedure can be found in previous papers.[12,13,22,23] We only like to mention here that

TABLE I. Layer dependent W atomic concentrations, C_j, and 5*d* total magnetic moments μ_j/atom (μ_B) for the Fe/W multilayer obtained from the simultaneous refinement of the experimental x-ray reflectivity and W L_3 XRMS results. Comparison with theoretical results for μ_j/atom.

Layer	Experiment		Theory	
j	C_j	μ_j	5Fe/7W[a]	5Fe/5W[b]
1	0.4	−0.377±0.017	−0.127	−0.136
2	0.8	0.063±0.015	0.025	0.019
3	1	−0.025±0.012	0.032	0.049
4	1	0.041±0.041	0	0.019
5	1	−0.017±0.014	0.032	−0.136
6	0.6	0.094±0.013	0.025	
7	0.3	−0.427±0.014	−0.127	

[a]5 ML Fe/7 ML W(001) multilayer with C_j=1 (Ref. 15).
[b]5 ML Fe/5 ML W(001) multilayer with C_j=1 (Ref. 15).

the number of atomic planes, their interplanar distances and the concentrations C_j are directly obtained from the analysis of the XRD and reflectivity data. In order to restrict as much as possible the number of free parameters, the structural parameters mentioned above were kept fixed during the refinement of the XRMS spectra. Furthermore, an additional constraint was added imposing that the average magnetic moment $\mu_{av}=\Sigma_j C_j\mu_j/\Sigma_j C_j$ in the W layer is equal to the one obtained from XMCD.

IV. DISCUSSION

The results of the simultaneous refinement of the asymmetry ratios, measured across the W L_3, are shown by the drawn curves in Fig. 4, and yield the W 5*d* induced magnetic profile presented in Table I for the different layers. We find that the W magnetic moment in the first layer at both interfaces is antiparallel to the Fe magnetic moment, which is $\sim 2\ \mu_B$. Interestingly, the W moment of the second layer is antiparallel to that of the first layer. The magnetization profile therefore shows a damped oscillation similar to that expected from the RKKY interaction. This tendency is in agreement with results from recent band-structure calculations,[15] which are reproduced in Table I for comparison. The theoretical results are for ideal interfaces without any roughness and give therefore a profile that is symmetric around the middle of the stack. This is clearly not the case for the experimental results (cf. Table I), where the interdiffusion at the two interfaces is different because W on Fe has a different growth than Fe on W. Furthermore, the measured W moments for the interface layers are much larger than the theoretical values. This increase in moment can be ascribed to the higher Fe coordination of the W atoms. This is supported by calculations, which find increased W moments for a 5 ML Fe/1 ML W multilayer [$-0.311\ \mu_B$ (Ref. 15)] and for W impurities in Fe [$-0.45\ \mu_B$ (Ref. 24)]. It is important to note that despite the unavoidable interface roughness and disorder the oscillatory behavior does not disappear. However, the damping is stronger and the period is shorter than in the ideal theoretical case that does not include interdiffusion.

Recently, Qian and Hübner[25] performed *ab initio* full-potential linearized augmented plane-wave calculations of 1 ML Fe on both W(100) and W(110). Since these calculations show a magnetic moment oscillation in 1 ML Fe/5 ML W(100) but not in 1 ML Fe/5 ML W(110), they would seem to be in apparent disagreement with our experimental results. However, we would like to emphasize several points indicating that a direct comparison between the results obtained for a multilayer and for a monolayer on a surface is ambiguous:

(i) The theoretical results for 1 ML of Fe on a W single crystal[25] cannot be directly compared with our multilayer result because of the huge difference from a structural point of view. While in the case of Fe(1 ML)/W, the Fe structure tends to adapt to the W bulk structure, the situation for a multilayer is more complicated. As shown by our XRD measurements on the multilayer, the thin W layer is contracted in-plane due to the thick Fe layer. Even though it could not be properly distinguished in a conventional XRD experiment, this strain is expected to be different for the two interfaces. The XRMS results (cf. Table I) clearly show strong differences between both interfaces. It is indeed one of the great strengths of our approach enabling us to distinguish the magnetic behavior of the two different interfaces.

(ii) The interdiffusion at the interfaces associated with the in-plane strain in the W layer does not justify a direct comparison based on the crystal structure and symmetry alone, however, it does allow the layer-by-layer type of comparison presented above. The capability to prepare high quality Fe/W multilayers (see e.g., the XRD reflectivity curves in Figs. 1 and 2) was of crucial importance because alloying at the interface is known to be an experimental limitation for the evidence of such a spin behavior.

(iii) The calculation by Qian and Hübner[25] does not include the spin-orbit coupling for the valence electrons. However, the calculations by Tyer *et al.*[15] show that the 5*d* spin-orbit coupling is rather important, resulting in an orbital moment that is about 20% and −40% of the spin moment for the first and second W layer, respectively.

(iv) While the calculation by Qian and Hübner[25] is done for a free-standing slab, the one by Tyer *et al.*[15] uses a "sandwich" structure that resembles the multilayer system. The study by Tyer *et al.* shows that the oscillatory spin oscillation can be understood as a consequence of the hybridization between the W 5*d* and Fe 3*d* states, which is mostly due to band filling, and to a lesser extent due to geometrical effects, such as the crystal structure (100 or 110) as singled out in the study of Qian and Hübner.[25]

V. CONCLUSIONS

We have used a combination of complementary x-ray based techniques to resolve experimentally the in-depth W 5*d* magnetization in Fe/W multilayers. X-ray anomalous reflectivity was used to obtain the multilayer period, the W and Fe layer thicknesses and the interface roughness. The crystallographic parameters have been extracted from x-ray diffraction at high angles. XMCD was used to obtain the mean

value of the induced W 5*d* polarization averaged over the W layer.

We have shown that, in addition to the detailed structural analyses combined with magnetic dichroism, the x-ray magnetic scattering in resonance with the W L_3 absorption can be utilized to resolve the W 5*d* magnetization profile. We have demonstrated the usefulness of this technique by verifying the existence of the recently predicted W 5*d* spin oscillations in Fe/W multilayers. We find the W magnetic moment in the first layer at both interfaces antiparallel to the Fe magnetic moment. Further, the moment of the second W layer is antiparallel to that of the first W layer. The magnetization profile shows a damped oscillation in agreement with recent results from band-structure calculations.[15] Despite the unavoidable interface roughness and disorder the oscillatory behavior does not disappear, however, the damping is stronger and the period is shorter than in the ideal theoretical case that does not include interdiffusion. We cannot confirm theoretical results predicting an absence of magnetic moment oscillations in 1 ML Fe/5 ML W(110).[25] This is primarily because, as shown by our XRD measurements, in the multilayer the thin W layer is contracted in-plane due to the thick Fe layer, making it structurally different from a monolayer on a surface.

The presented results open the way for further studies of periodic magnetic nanostructures containing 5*d* metals, of high potential interest for GMR, where XRMS measures the weak induced 5*d* magnetization, independently from the large 3*d* transition metal moments. XRMS offers a large sampling depth ideal for buried interfaces and can be performed in the presence of externally applied magnetic and electric fields. The use of the kinematical approximation which proved to work in the specific case of multilayers, allows us to use a rather simple refinement procedure to obtain the magnetization of the probed atom in each atomic plane without having to assume a specific model. We would like to point out, that such an approach using diffraction peaks provided by the chemical modulation of the multilayer can be extended to the soft x-rays range, even though the accessible reciprocal space is restricted, however, at the expense of having to use dynamical diffraction theory.

[1] F. de Bergevin and M. Brunel, Phys. Lett. **39A**, 141 (1972).
[2] M. Blume, J. Appl. Phys. **57**, 3615 (1985).
[3] K. Namikawa, M. Ando, T. Nakajima, and H. Kawata, J. Phys. Soc. Jpn. **54**, 4099 (1985).
[4] D. Gibbs, D. R. Harshman, E. D. Isaacs, D. B. McWhan, D. Mills, and C. Vettier, Phys. Rev. Lett. **61**, 1241 (1988).
[5] E. D. Isaacs, D. B. McWhan, C. Peters, G. E. Ice, D. P. Siddons, J. B. Hastings, C. Vettier, and O. Vogt, Phys. Rev. Lett. **62**, 1671 (1989).
[6] J. P. Hannon, G. T. Trammell, M. Blume, and D. Gibbs, Phys. Rev. Lett. **61**, 1245 (1988).
[7] B. T. Thole, G. van der Laan, and G. A. Sawatzky, Phys. Rev. Lett. **55**, 2086 (1985).
[8] G. van der Laan, B. T. Thole, G. A. Sawatzky, J. B. Goedkoop, J. C. Fuggle, J. M. Esteva, R. Karnatak, J. P. Remeika, and H. A. Dabkowska, Phys. Rev. B **34**, 6529 (1986).
[9] C. Kao, J. B. Hastings, E. D. Johnson, D. P. Siddons, G. C. Smith, and G. A. Prinz, Phys. Rev. Lett. **65**, 373 (1990).
[10] J. M. Tonnerre, L. Sève, D. Raoux, G. Soullié, B. Rodmacq, and P. Wolfers, Phys. Rev. Lett. **75**, 740 (1995).
[11] H. A. Dürr, E. Dudzik, S. S. Dhesi, J. B. Goedkoop, G. van der Laan, M. Belakhovsky, C. Mocuta, A. Marty, and Y. Samson, Science **284**, 2166 (1999).
[12] L. Sève, N. Jaouen, J. M. Tonnerre, D. Raoux, F. Bartolomé, M. Arend, W. Felsch, A. Rogalev, J. Goulon, C. Gautier, and J. F. Bérar, Phys. Rev. B **60**, 9662 (1999).
[13] N. Jaouen, J. M. Tonnerre, D. Raoux, E. Bontempi, L. Ortega, M. Muenzenberg, W. Felsch, A. Rogalev, H. A. Dürr, E. Dudzik, G. van der Laan, M. Suzuki, and H. Maruyama, Phys. Rev. B **66**, 134420 (2002).
[14] N. Ishimatsu, H. Hashizume, S. Hamada, N. Hosoito, C. S. Nelson, C. T. Venkataraman, G. Srajer, and J. C. Lang, Phys. Rev. B **60**, 9596 (1999).
[15] R. Tyer, G. van der Laan, W. M. Temmerman, Z. Szotek, and H. Ebert, Phys. Rev. B **67**, 104409 (2003).
[16] F. Wilhelm, P. Poulopoulos, H. Wende, A. Scherz, K. Baberschke, M. Angelakeris, N. K. Flevaris, and A. Rogalev, Phys. Rev. Lett. **87**, 207202 (2001).
[17] E. E. Fullerton, J. Pearson, C. H. Sowers, S. D. Bader, X. Z. Wu, and S. K. Sinha, Phys. Rev. B **48**, 17 432 (1993).
[18] J. Goulon, A. Rogalev, C. Gautier, C. Goulon-Ginet, S. Paste, R. Signorato, C. Neumann, L. Varga, and C. Malgrange, J. Synchrotron Radiat. **5**, 232 (1998).
[19] B. T. Thole, P. Carra, F. Sette, and G. van der Laan, Phys. Rev. Lett. **68**, 1943 (1992).
[20] P. Carra, B. T. Thole, M. Altarelli, and X. Wang, Phys. Rev. Lett. **70**, 694 (1993).
[21] J. M. Tonnerre, *X-Ray Magnetic Scattering in Magnetism and Synchrotron Radiation*, edited by E. Beaurepaire, B. Carrière, and J. P. Kappler (Les Éditions de Physique, Les Ulis, 1996), p. 245.
[22] N. Jaouen, J. M. Tonnerre, D. Raoux, L. Ortega, E. Bontempi, M. Muenzenberg, W. Felsch, M. Suzuki, H. Maruyama, H. A. Dürr, E. Dudzik, and G. van der Laan, Appl. Phys. A: Mater. Sci. Process. **73**, 711 (2001).
[23] N. Jaouen, J. M. Tonnerre, D. Raoux, M. Muenzenberg, W. Felsch, A. Rogalev, N. B. Brookes, H. A. Dürr, and G. van der Laan, Acta Phys. Pol. B **34**, 1403 (2003).
[24] R. Tyer, G. van der Laan, W. M. Temmerman, and Z. Szotek, Phys. Rev. Lett. **90**, 129701 (2003).
[25] X. Qian and W. Hübner, Phys. Rev. B **67**, 184414 (2003).